UCRL-92311
PREPRINT

Gamma Radiation Effects on Corrosion: I Electrochemical Mechanisms for the Aqueous Corrosion Processes of Austenitic Stainless Steels

Robert S. Glass
George E. Overturf III
Richard A. Van Konynenburg
R. Daniel McCright

Radiation Physics and Chemistry

February 1985

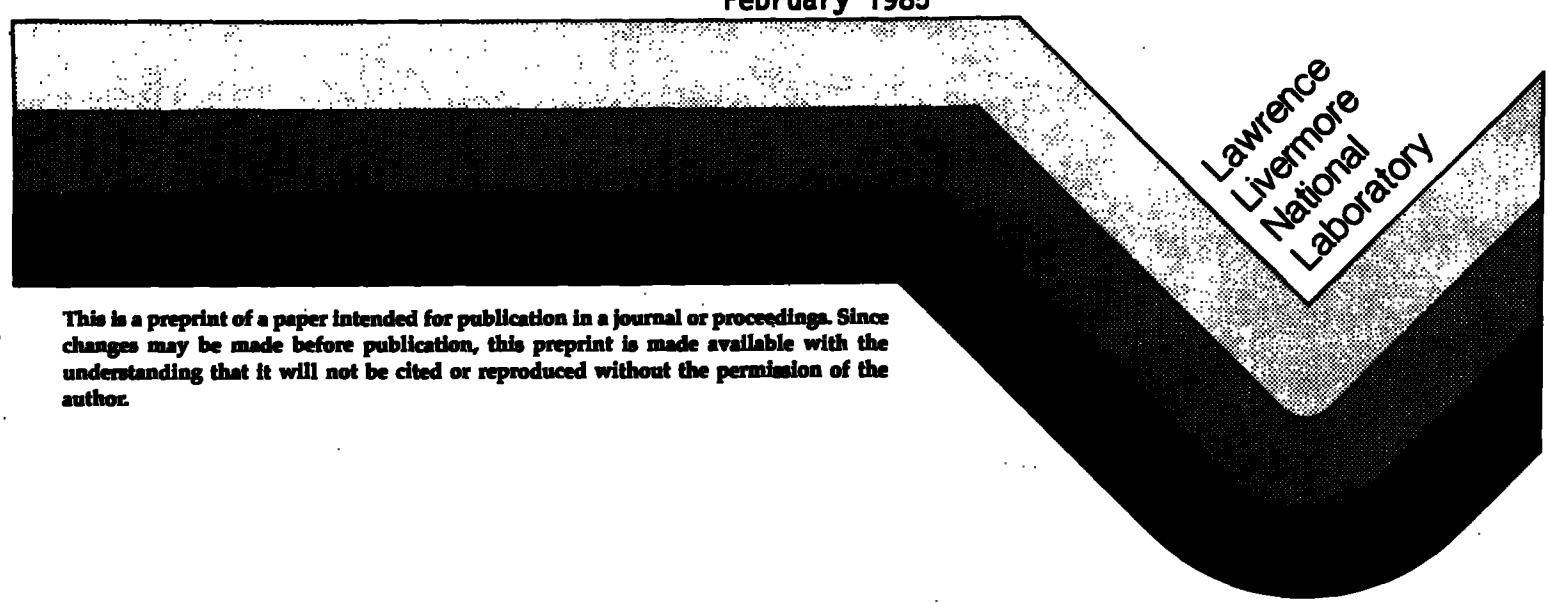

Gamma Radiation Effects on Corrosion, I. Electrochemical Mechanisms for the Aqueous Corrosion Processes of Austenitic Stainless Steels

Robert S. Glass, George E. Overturf III,
Richard A. Van Konynenburg, and R. Daniel McCright

Lawrence Livermore National Laboratory
Livermore, CA 94550

Abstract

The Nuclear Regulatory Commission regulations for geologic disposal of high level nuclear wastes require multibarriered packages for waste containment that are environmentally stable for time periods of 300 to 1000 years. In addition to examining the usual corrosion failure modes which must be evaluated in choosing a corrosion resistant material for waste containment (e.g., resistant to pitting, crevice attack, and stress-corrosion cracking), the effects of gamma radiation on the chemical environment surrounding the waste container must also be considered. Austenitic stainless steels have been proposed for use as waste container materials for a potential nuclear waste repository to be located at Yucca Mountain in Nye County, Nevada. This study focuses on the effects of gamma radiation on the corrosion mechanisms of 316L stainless steel in groundwater regional to this site. When gamma irradiation is initiated, corrosion potential shifts in the positive direction are observed for 316L in groundwater regional to the repository site. These potential shifts are associated with the radiation-induced production of hydrogen peroxide. The electrochemical mechanisms involved in the corrosion potential shifts, as well as the subsequent effect on pitting resistance, are considered.

---

*Work performed under the auspices of the U.S. Department of Energy by the Lawrence Livermore National Laboratory under contract number W-7405-ENG-48 as part of the Nevada Nuclear Waste Storage Investigations.

Introduction

The safe disposal of high level nuclear waste materials in geological media represents a current technological challenge. One aspect of this challenge is the development of barrier packages that must be environmentally stable for time periods of 300 to 1000 years. In designing metallic engineered barriers for waste disposal, the susceptibility to potential corrosion failure modes such as uniform corrosion, pitting, crevice attack, hydrogen embrittlement, and stress-corrosion cracking must be evaluated. In addition to these failure modes normally encountered in corrosion studies, the interaction of gamma radiation from the waste with the surrounding chemical environment must be understood in light of possible effects on corrosion mechanisms.

The interaction of gamma radiation with aqueous environments produces a host of transient radicals, ions, and stable molecular species including $H\cdot$, $\cdot OH$, e^-_{aq}, H_3O^+, OH^-, H_2, H_2O_2, O_2, O_2^-, and HO_2.[1-3] Species such as e^-_{aq}, $H\cdot$, and H_2 can act as reducing agents, while others such as H_2O_2, $\cdot OH$, O_2, O_2^- and HO_2 can act as oxidizing agents. As a result of the production of such species under gamma irradiation, there may be alterations in the rates or mechanisms of corrosion attack modes.

Previous investigations have found an increased susceptibility of sensitized 304 stainless steel towards intergranular stress corrosion cracking in high temperature water under gamma irradiation.[4,5] Other reports have claimed an increased resistance to crevice corrosion for austenitic stainless steels in aqueous solutions under gamma irradiation.[6] For carbon steel and 304 stainless steel, gamma irradiation in high temperature (250°C) water containing low oxygen levels has been shown to increase the release rates of insoluble corrosion products (crud) but not to increase the release rates of soluble products.[7]

Several reports have demonstrated effects of gamma irradiation on the corrosion potentials of austenitic stainless steels in aqueous media.[6, 8-11] Some of this work has been performed in acidic media where a complicated corrosion potential behavior is observed that reflects a balance between the reducing and oxidizing species generated under radiolysis and the

experimental condition (e.g., aeration vs. deaeration). Shifts of the corrosion potential in the positive direction have generally been observed under gamma irradiation of oxygenated aqueous systems.

In general, a fundamental understanding of the effect of gamma irradiation on the mechanisms of corrosion of austenitic stainless steels is lacking. In particular, in near-neutral aqueous environments, the introduction of new electrochemical reactions by the radiolytically-generated oxidants has received little mechanistic investigation. However, species such as H_2O_2, O_2, HO_2, O_2^-, etc. which are generated radiolytically, are generally assumed to increase the oxidizing nature of the environment.

The effects of gamma irradiation on waste package corrosion mechanisms in environments relevant to proposed nuclear waste repository sites are just beginning to be explored. One site under current consideration for a potential nuclear waste repository is located in Yucca Mountain adjacent to the Nevada Test Site. Although the repository horizon at this site would be in densely welded tuff above the static water table, intrusions of vadose water could occur from matrix flow through the rock or episodically through fractures in the rock. The low annual precipitation at the site and low rate of percolation of this water downward minimizes the actual amount of water entering the waste package environment. The heat generated from the nuclear waste will vaporize incoming water at temperatures above 95°C (boiling point of water at the repository elevation). For the large majority of waste packages, container surface temperatures are estimated to remain above 95°C for several hundreds of years.[12] For this repository location, austenitic stainless steels (e.g., 304L, 316L) have been proposed for use as waste canister materials.[13]

In addition to groundwater containing naturally occurring concentrations of dissolved species, it is also of interest to consider solutions in which these species are more concentrated. Evaporative processes at the repository site could lead to concentration of the electrolyte. Such concentrated solutions could arise since groundwater may intrude into the repository site prior to the time that the container surface has cooled to below boiling temperature and then evaporate and leave behind salt deposits. Subsequent

repetition of these events at the same locations could conceivably result in local salt build-up. When the container surface temperature has cooled to below the boiling point, further wetting at locations of salt build-up could lead to a concentrated electrolyte. This concentrated electrolyte could only result from a sequence of low probability events; however, observing the performance of candidate container materials under such environmental conditions is instructive and is also necessary for selection of a successful candidate material that will meet regulatory requirements for long-term integrity of the container.

In this paper, initial results are reported on the in-situ electrochemical characterization of the response of 304L and 316L to gamma-irradiated groundwater that is regional to the potential tuff repository site. Open-circuit potential measurements and anodic polarization curves were obtained under gamma irradiation. The major species responsible for the observed electrochemical changes is shown to be radiolytically-generated H_2O_2. Initial assessment of the effect of radiolysis on corrosion mechanisms (e.g., pitting resistance) of 316L is given. The electrochemical mechanisms leading to the observed corrosion potential behavior under gamma irradiation are explored. Despite the fact that this study was site-specific, the principal mechanisms and the general results should be applicable to any near-neutral (or somewhat alkaline) aqueous system with low concentrations of solute species.

Experimental

Austenitic stainless steels 304L and 316L were used in the solution annealed condition. The compositions of the alloys used are given in Table 1. Rods of these materials 0.318 cm in diameter by 15.2 cm in length were used as working electrodes. All samples were polished with the sequence 600 grit SiC, 5μ, 1μ, 0.3μ and ending in 0.05μ Al_2O_3 slurries prior to use.

The groundwater used in these experiments was obtained from well J-13, which is located near the repository site. The J-13 well penetrates the water table at a lower elevation than that of the proposed repository site. Water

from this well has percolated through the densely welded tuff layer proposed for the repository. The composition of the groundwater is shown in Table 2. Analyses of the constituents were made by ion chromatography and inductively-coupled plasma emission spectroscopy. In some experiments, concentrated forms of this groundwater (10x and 100x) were used. Boil-down under atmospheric pressure was used to obtain the more concentrated electrolytes. When additions of other species were made, analytical reagent chemicals (H_2O_2 and NaCl) or ultra-high purity gases (H_2 and O_2) were used. Unless otherwise indicated all experiments were performed in initially air-saturated solutions vented to the atmosphere.

A diagram of the electrochemical apparatus used in this work is shown in Figure 1. The reference electrode (SCE) is placed in a reservoir containing saturated KCl in the upper chamber. The upper and lower chambers are connected by a Luggin probe, approximately 1.4 m long, filled with saturated KCl. The lower chamber, which is the only part of the system surrounded by the gamma sources, contains the Pyrex electrochemical cell. The cell itself has inlets for the reference electrode Luggin probe, the working electrode, a coiled Pt-wire counter electrode and a port for deaeration. In this arrangement the reference electrode is isolated from the gamma sources.

The gamma sources consisted of ^{60}Co pencils in a cylindrical arrangement. The lower chamber of the electrochemical cell was inserted into the inside of this cylinder, at the center of which the dose rate was 3.3 Mrad/hr ($\pm$20%). All experiments were performed at 30°C ($\pm$5°C).

Open-circuit potential vs. time and anodic polarization curves were obtained with the aid of a Princeton Applied Research Model 173 potentiostat and Model 176 current-to-voltage converter. Steady-state polarization curves were obtained using the potential step method. Here, the working electrode potential was sequentially stepped in the positive direction in increments of 20-30 mV starting from the corrosion potential. The current was then monitored until a steady-state was achieved. The current-potential relationship was then output to an x-y recorder, and the next potential programmed into the potentiostat.

Results and Discussion:

Aqueous Environment and Radiation Chemistry:

As noted above, Table 2 represents the composition of groundwater which is regional to the proposed repository site. The low concentrations of solute species, particularly the detrimental anion Cl^-, and the near-neutral pH (7.6) suggest that this electrolyte should be relatively benign with regard to corrosion of austenitic stainless steels.

Before proceeding to interpret the electrochemical experiments, it is helpful to consider what is known about bulk radiation chemistry of aqueous solutions from past work in this field. Because the groundwater contains only low concentrations of solutes, its bulk radiation chemistry should be very similar to that of pure water. In pure, deaerated water the primary radiolytic species under gamma irradiation are $H\cdot$, $\cdot OH$, e^-_{aq}, H_3O^+, OH^-, H_2, H_2O_2, and HO_2.[2] In an inert, closed vessel these species undergo reactions with each other to reform water, resulting in small steady-state concentrations of radicals and molecular species, and no further decomposition of water. The species having the highest concentrations are H_2, O_2, and H_2O_2.[14]

If the water contains a few ppm of dissolved oxygen, the reducing species $H\cdot$ and e^-_{aq} are rapidly converted to HO_2 and O_2^-, respectively. If the pH is greater than about 4.5, the HO_2 ionizes to form additional O_2^-.[15] In the case of oxygenated water, H_2 and $H\cdot$ are suppressed, and the most abundant species are O_2 and H_2O_2.[14] At the proposed repository site, the J-13 well water would be in equilibrium with air and would therefore contain several ppm of O_2.[12, 13, 16]

The pH region from 7 to 10 is of the most interest for J-13 well water. With evaporation and concentration of this electrolyte (i.e., to 100x concentration), calcium silicate and carbonate precipitate and the pH rises to around 10. The geochemistry of the regional J-13 well water has been thoroughly discussed by Oversby.[16] The yields (G-values) of the primary species in the radiolysis of pure water are roughly independent of pH in the

region from pH 4 to 10.[2] Under radiolysis of J-13 well water we can therefore expect an oxidizing environment with O_2 and H_2O_2 as the dominant species, a smaller concentration of O_2^-, and much smaller steady-state concentrations of H_2, $\cdot OH$, and $H\cdot$. It should be noted that we do not expect significant production of nitric acid in these experiments because of the small air volume and the short duration of the experiments. Under worst-case conditions in our experiments we would expect a maximum concentration of approximately 1.6×10^{-5} M. A sample calculation, based upon the results of Burns et. al.,[17] is given in Appendix I. Under repository conditions, HNO_3 production is expected to be more important. The effects of the radiolytic species on electrochemical mechanisms will be outlined in the following discussion.

Electrochemical Potential Measurements

The corrosion potential (the terms "open-circuit potential" and "E_{oc}" are also used interchangeably in this paper) of austenitic steels is significantly affected by gamma irradiation due to the generation of new oxidizing species. Upon imposition of the gamma field, the corrosion potential of both 304L and 316L in a series of electrolytes related to J-13 well water shifted in the positive direction, typically by 150-200 mV. Such results are shown for 316L in 10x and 100x concentrated J-13 in Figures 2 and 3, respectively. In these figures, "on" refers to lowering of the cell into the center of the gamma sources and "off" refers to raising the cell 1.3 to 1.5 m above the sources where the cell would be shielded by intervening water. Several "on/off" cycles are shown. Similar positive potential shifts upon imposition of the gamma field were observed for 316L in non-concentrated J-13 well water and when 304L was the electrode material.

From these experiments, it seems clear that the positive potential shifts in the corrosion potential resulted from the more oxidizing environment produced by gamma irradiation. Such potential shifts may be generic to austenitic stainless steels, since the same behavior was observed with both 304L and 316L in J-13 well water and its more concentrated forms. As will be discussed more fully below, the initial rapid rise of potential upon imposition of the gamma field is likely the result of the generation of

oxidizing •OH radicals and/or H_2O_2 in the solution layers next to the electrode surface. The subsequent slower rise of potential with time corresponds to the slower buildup of the steady-state bulk concentration of H_2O_2. The fall in potential upon removal from the gamma field likely results from the discontinuation of the production of •OH radicals in the solution layers next to the electrode surface. The potential does not, however, return to the pre-radiolysis values, because a stable concentration of H_2O_2 has been formed in solution.

Following several "on/off" cycles the cells containing 304L or 316L specimens were removed from the gamma facility and the open-circuit potential was monitored for several hours (generally more than 14 hours). The potential remained at the high (relative) positive values which were induced by gamma irradiation. These results indicated either permanent changes in the oxide films on the electrodes, or the generation of a stable concentration of oxidizing species in solution, or both.

In order to test whether the observed effects resulted from stable oxidizing species produced in the solution or from permanent changes in the oxide film on the electrode, the following experiment was performed: Following several "on/off" cycles for 316L stainless steel in J-13 water, the cell was removed from the gamma facility and the irradiated solution was replaced by "fresh" non-irradiated J-13 water. When this was done, the corrosion potential immediately shifted in the negative direction (see Figure 4). This indicates that the positive potential shifts observed are due principally to radiolytically-generated stable oxidizing species rather than to oxide film changes. If the latter had been the case, the oxide layer would not have been expected to change back to its original state when the solution was replaced, particularly not as rapidly as the observed change in potential occurred.

To see whether H_2O_2 alone could produce the potential shifts of the magnitude observed under irradiation, one drop of 30% H_2O_2 solution was added to the fresh J-13 water in the cell from the experiment above, producing a concentration of 4.8 mM. The potential was observed to shift in the positive direction immediately (see Figure 4). The observed change when

H_2O_2 was added to the solution, coupled with the knowledge that H_2O_2 is the most concentrated radiolytic species present in an irradiated, aerated solution, provides strong evidence that it is responsible for the potential shift observed upon irradiation in these solutions.

In a similar experiment, successive additions of 30% H_2O_2 solution were made to an unirradiated J-13 solution in which a freshly prepared 316L electrode was immersed. The results of this experiment are shown in Figure 5. In this figure, a one drop addition to the solution represents a concentration increase of approximately 0.49 mM. This value is within a factor of four of the value 0.14 mM which we measured for H_2O_2 in irradiated solution following 3.5 hours exposure, using the titanium oxalate method.[18] It can be seen that the potential shift observed following the addition of the first drop is within the range of potential shifts observed under radiolysis (150-200 mV). Successive addition of H_2O_2 (at the breaks in the curve) yield smaller potential jumps than the initial addition on a per-drop basis, indicating a tendency toward an eventual saturation point. In each successive one-drop addition, the concentration of H_2O_2 increases by 0.49 mM. These results add further support to the interpretation that the production of H_2O_2 under radiolysis leads to the long-term potential shifts observed.

To shed further light on the electrochemical effects of irradiation, and to separate possible electrode effects from solution effects, we performed some experiments using smooth platinum as the working electrode. In contrast to the behavior observed for austenitic stainless steels under irradiation, smooth Pt in J-13 well water shows quite different behavior as shown in Figure 6. Upon initiation of irradiation the open-circuit potential immediately drops to more negative values.

The very different results for platinum can be understood as follows: Pt, as an electrode, will be very responsive to the presence of $H^\bullet$ and H_2, which are also produced in radiolysis. In the bulk of the solution, $H^\bullet$ is expected to react rapidly with O_2, as stated above, and to have a very low steady-state concentration. However, near the electrode surface, it should be available for interfacial reactions. Likewise H_2, though present at small

concentration in the bulk and normally not very reactive in aqueous solutions at room temperature, can be an important factor at the surface of a Pt electrode, which is catalytic to H_2. The E_{oc} for Pt thus tends toward the potential of a "hydrogen electrode" to the degree allowed by the steady-state concentrations of all the species produced by irradiation. The cathodic spikes observed in the "on/off" cycles possibly indicate a greater transient concentration of H• and/or H_2 at the electrode surface. The drop in potential observed upon termination of irradiation is probably due to the rapid decrease in •OH concentration,[14] while H_2 remains as a stable species. The subsequent rapid increase in E_{oc}, producing the spike, may be due to the depletion of H_2 from the region near the Pt, so that the effects of the remaining H_2O_2 can be seen. This could be facilitated by catalytic decomposition of H_2 to H• by the Pt, followed by reaction of H• with H_2O_2. Since the steady-state H_2 concentration in an irradiated, oxygenated solution is much smaller than that of H_2O_2, the H_2 could thus be depleted easily, leaving considerable H_2O_2 in the solution to affect the potential, which would shift the E_{oc} in the positive direction.

In the second Pt experiment, we bubbled argon through the solution before and during irradiation to remove oxygen and inhibit, although not eliminate completely, the formation of bulk H_2O_2. The results of this experiment are shown in Figure 7. In this case, the spikes and the corresponding potentials in "on/off" cycles were more negative than those corresponding to the air-saturated experiment above. This indicates an enhanced response to the reducing species H• and H_2 when formation of the oxidizing species H_2O_2 is inhibited. In summary, Pt appears to be more responsive to H• and H_2 than to H_2O_2.

The response of Pt in unirradiated J-13 water with additions of H_2O_2 and H_2 is shown in Figure 8. Again, the much greater response of Pt to H_2 (it assumes the E_{oc} value for the "hydrogen" electrode at pH ≈7) than H_2O_2 is evident when the H_2 purging of the solution is initiated. When the solution is subsequently purged with O_2, removing the H_2 from the saturated solution, the potential recovered to near its value before H_2 was added.

This experiment was repeated using a 316L stainless steel electrode, producing the results shown in Figure 9. When two drops of 30% H_2O_2 solution were added, producing a concentration of 0.98 mM, the open-circuit potential immediately shifted positively. Upon subsequently purging the solution with H_2, however, 316L showed no response. The contrast between the behavior of platinum and that of 316L stainless steel is thus very dramatic and indicates that the 316L electrode, with an oxide film formed under our conditions, acts as a poor "hydrogen" electrode and is believed to have a low rate constant for dissociation of H_2 on its surface. However, the response of this material to H_2O_2 is dramatic. This is instructive from the point of view that H_2 is also a stable molecular product of radiolysis. Although 316L is not significantly affected by molecular H_2, the response to radiolytically-generated atomic hydrogen produced in the solution layers immediate to the electrode surface has not been determined.

Previous investigations have shown decreased levels of H_2O_2 produced under gamma radiolysis when inert gases were used to purge the system during radiolysis.[19, 20] Argon bubbling inhibits the bulk formation of H_2O_2 via the removal of O_2 from the system, which inhibits reactions forming H_2O_2. Nevertheless, the corrosion potential in our experiments still shifted positively when argon purging was employed prior to, and throughout irradiation of a 316L electrode in J-13 well water, as shown in Figure 10. While argon bubbling inhibits (but does not eliminate) bulk H_2O_2 formation, it appears that under gamma radiolysis the steel electrode still responds to the formation of •OH and H_2O_2 in solution. While purging of the solution with argon inhibits the formation of H_2O_2, it will not inhibit the formation of •OH radicals. The production of the transient •OH species in the solution layers adjacent to the electrode can lead to an increase in the oxidizing nature of the environment at the electrochemical interface, and hence to positive corrosion potential shifts. The probable electrochemical mechanisms at stainless steel interfaces involving •OH and H_2O_2 will be examined below.

Electrochemical Mechanisms:

A large number of electrochemical reactions involving oxidizing species are possible in gamma-irradiated aqueous solutions. Some of these are listed in Table 3.[2, 21] Of course, the corrosion potential will be a mixed potential resulting from the superposition of the kinetics of all the anodic and cathodic reactions occurring on the surface. The situation is so complex that the relative contributions of reactions of secondary importance are difficult to ascertain. The relative importance of the reactions shown in Table 3 will depend upon such factors as dose rate, pH, relative concentrations, electron transfer rate constants, temperature, relative concentrations of "scavenger" species, etc.

In considering the electrochemical behavior of Pt in non-irradiated aqueous solutions of H_2O_2, Bockris and Oldfield[22] proposed the following reaction as determining the open-circuit potentials observed:

$$(\cdot OH)_{ads} + e^- \rightleftarrows OH^- \qquad (1)$$

In this equation, adsorbed hydroxyl radicals on the Pt surface participate in an electrochemical equilibrium with hydroxide ions in solution. The adsorbed hydroxyls originate from a surface-catalyzed decomposition of H_2O_2, i.e.,

$$H_2O_2 \xrightarrow{Pt} 2(\cdot OH)_{ads} \qquad (2)$$

In their work, the pH dependence of the open-circuit potential of Pt was given as

$$E_{oc,Pt} = 0.594 - 0.059\ pH \quad \text{volts vs. SCE.} \qquad (3)$$

The potential was found to be independent of the concentration of H_2O_2 down to 10^{-6} M. At concentrations above this value, a saturation surface coverage of hydroxyl radicals was postulated. At a pH of 7, the E_{oc} value for Pt would therefore be 0.181 V vs. SCE. At incomplete surface coverages, more negative potentials were observed. Since their work was performed in high-purity aqueous solutions of H_2O_2, one would not necessarily expect

the same potential dependence in J-13 well water, which contains ppm levels of such other solute species as NO_3^-, SO_4^{-2}, HCO_3^-, etc., which may also influence interfacial kinetics.

Subsequent to this work, R. Gerischer and H. Gerischer proposed a more complicated scheme to explain the electrochemical behavior of Pt in aqueous solutions of H_2O_2.[23] In their scheme, H_2O_2 was conceived to be electrochemically discharged on Pt into either adsorbed hydroxyl or perhydroxyl (HO_2) radicals in cathodic or anodic reactions, respectively. With a relative importance depending upon pH, the adsorbed hydroxyls could then participate in a cathodic process to liberate OH^-, whereas the adsorbed HO_2 species could liberate O_2 by an anodic process. In addition, and concurrently, these adsorbed species •OH and HO_2 could participate in a cyclical catalytic mechanism to decompose H_2O_2 on the surface, liberate H_2O and O_2, and regenerate the original adsorbed species (•OH and HO_2). This catalytic scheme would be more important at higher pH. The balance of anodic and cathodic reactions in this cyclical catalytic scheme would then determine the open-circuit potential for Pt.

In the case of gamma radiolysis where both •OH and H_2O_2 are generated in solution and may directly adsorb or decompose on the surface, respectively, either of the above mechanisms could be important in determining the corrosion potential of austenitic stainless steels. These species, generated in the solution layers next to the electrode, would be important in this regard. In the bulk, only the generation of H_2O_2 will be important as the •OH radicals have too short a lifetime to diffuse appreciably.[2, 3, 14] As stated previously, the generation of both •OH and H_2O_2, particularly •OH, in the solution layers next to the electrode are probably important for the initial rapid rise in potential observed upon imposition of the gamma field. The subsequent slower rise of potential is probably due to the bulk generation of H_2O_2 and its diffusion to the electrode surface. If the Gerischer mechanism for H_2O_2 decomposition can be applied to the behavior of austenitic steels in aqueous solution under irradiation, another oxidizing species, O_2, could also be present at the electrode surface. The corrosion potential would then be established by a balance of the anodic and cathodic processes occurring in the cyclical catalytic decomposition of H_2O_2.

Although reactions such as (1) and (2), or, alternatively, the catalytic mechanism of Gerischer and Gerischer, may be very important in determining the corrosion potential of austenitic stainless steels in aqueous solution under gamma radiolysis, the situation is complex in that other reactions (e.g., metal dissolution) will also certainly play a role. Stainless steel forms a much more complex electrochemical interface with aqueous solutions than does Pt and may not have a surface saturation coverage of adsorbed hydroxyl species. A lower rate constant for the decomposition of H_2O_2, or other reactions with the oxide film may account for this. In any case, one would not a-priori expect the same open-circuit potential behavior for austenitic stainless steels under gamma irradiation as is observed for Pt in non-irradiated aqueous solutions of H_2O_2. The mechanisms leading to the positive corrosion potential shifts for austenitic stainless steel under gamma irradiation, although clearly associated with the production of •OH and H_2O_2, need further clarification.

The anodic and cathodic reactions which are believed to be of major importance in determining the corrosion potentials of austenitic stainless steels under gamma irradiation are listed below. Based upon the results presented above, we believe that these reactions will probably predominate under gamma irradiation in aerated aqueous systems similar to those of J-13 well water and its concentrated (10x, 100x) forms when the pH is neutral to mildly alkaline.

Cathodic reactions:

$$(\bullet OH)_{ads} + e^- \rightleftarrows OH^- \qquad (4)$$

$$O_2 + 2H_2O + 4e^- \rightarrow 4OH^- \qquad (5)$$

$$O_2^- + H_2O + e^- \rightarrow HO_2^- + OH^- \qquad (6)$$

(small contribution)

$$HO_2^- + H_2O + 2e^- \rightarrow 3OH^- \quad (7)$$
(very small contribution)

Anodic reactions:

$$Fe \rightarrow Fe^{+2} + 2e^- \quad (8)$$

$$Cr \rightarrow Cr^{+3} + 3e^- \quad (9)$$

$$Ni \rightarrow Ni^{+2} + 2e^- \quad (10)$$

$$2OH^- + H_2O_2 \rightarrow O_2 + 2H_2O + 2e^- \quad (11)$$
(small contribution at higher pH)

$$HO_2^- + OH^- \rightarrow O_2 + H_2O + 2e^- \quad (12)$$
(small contribution at higher pH)

The last two reactions for both the cathodic and anodic sets are expected to be of lesser importance at near-neutral pH. The coupling of the cathodic processes with metal dissolution reactions will result in the observed mixed corrosion potential. Again, the equilibrium described in equation (1) may be one of the most important reactions pinning the corrosion potential.

Along with the surface reactions, the radiolytically generated species can also participate in a series of bulk oxidation reactions such as those given in reactions (13) through (18).

$$\cdot OH + Fe^{+2} \rightarrow Fe^{+3} + OH^- \quad (13)$$

$$HO_2 + Fe^{+2} \rightarrow Fe^{+3} + HO_2^- \quad (14)$$

$$H_2O_2 + Fe^{+2} \rightarrow Fe^{+3} + OH^- + \cdot OH \quad (15)$$

$$H\cdot + Fe^{+2} \rightarrow Fe^{+3}H^- \quad (16)$$

$$Fe^{+3}H^{-} + H^{+} \rightarrow Fe^{+3} + H_2 \quad (17)$$

$$2Fe(OH)_2 + H_2O_2 \rightarrow 2FeOOH + 2H_2O \quad (18)$$

Processes such as the oxidation of ferrous ion under gamma radiolysis have been proposed previously to explain an observed inhibition of crevice corrosion of stainless steels.[6]

In addition to the above reactions, the radiolytic species may also participate in film formation or repair reactions of the nature of those below.[6]

$$xMe + yOH \rightarrow Me_x(OH)_y \quad (19)$$

$$xMe + yHO_2 \rightarrow Me_xO_{1.5y}0.5yH_2O \quad (20)$$

Localized Corrosion Effects

For practical applications, it is important to know what the effect of the positive corrosion potential shifts will be on the corrosion mechanism(s). In particular, we would like to find out whether the positive potential shifts increase the susceptibility of the material to pitting. Polarization curves are helpful in resolving this question.

Initial results appear to indicate that the pitting susceptibility of 316L is not increased under gamma irradiation. This is shown by comparison of the steady-state polarization curves in Figure 11 obtained both in-situ in the gamma field and ex-situ in unirradiated solution. The solution used in this case was 650 ppm Cl^- in distilled water. This solution represents a 100-fold increase in concentration of this particularly detrimental anion with respect to J-13 well water, and should be more conducive to pitting.

For the non-irradiated case, the corrosion potential (given by the intersection of the curve with the y-axis) was -110 mV (vs. SCE). Upon scanning anodically, the pitting potential was found to be 220 mV, as identified by the intersection of the extrapolated lines from the passive and

pitting regions of the curve. (The pitting potential is defined as the potential at which the protective oxide film breaks down locally and a sudden increase in current density is observed.[24]) The value of $E_{pit} - E_{corr}$ is therefore 330 mV. For the gamma irradiation case, the corresponding values for E_{corr} and E_{pit} are 50 mV and 390 mV. This represents a separation of $E_{pit} - E_{corr}$ of 340 mV.

It therefore appears that both the corrosion potential and the pitting potential are shifted positively in the presence of gamma radiolysis, and by roughly the same amount. Since the separation of these two values remains essentially the same as it is without gamma irradiation, there appears to be no increase in susceptibility to pitting with gamma irradiation. As observed from the agreement of the latter portions of the polarization curves in the reverse cathodic scans, there also appears to be no effect of gamma irradiation on the repassivation potential (around 0 V for each case). The repassivation potential represents the point at which the growth of the pits which were produced by anodic polarization is inhibited.[24] Experimentally, it is identified as the potential at which the current tends toward zero on the reverse scan. It must be emphasized that the polarization behavior shown here represents initial results, and much further work is required to understand the effect of gamma irradiation over a wide potential range. The beneficial effect of gamma irradiation as observed in the more positive pitting potential may result from reaction of the radiolytic species with the passive oxide film. Such reactions could work to heal lattice defects such as oxygen vacancies, or could result in film repair reactions such as those in reactions (19) and (20).

Conclusions

1. Gamma irradiation increases the oxidizing nature of the aqueous solutions used in this study through production of $\cdot OH$ and H_2O_2. These species probably account for the observed positive corrosion potential shifts. Such shifts may be generic for austenitic stainless steels in J-13 well water and in similar environments.

2. By analogy to previous work on Pt in aqueous H_2O_2 media, the electrochemical equilibrium between adsorbed hydroxyl species and hydroxide ions may be important in determining the corrosion potentials of stainless steel in irradiated aqueous solutions. Also a cyclical catalytic scheme for the decomposition of H_2O_2 involving adsorbed species (e.g., $\cdot OH$, HO_2, or O_2^-) participating in anodic and cathodic processes may also be important. However, a stainless steel surface certainly forms a more complex electrochemical interface than does a Pt surface, and other reactions also serve to establish a mixed corrosion potential, as discussed in the text.

3. The generation of oxidizing species in the solution layers adjacent to the stainless steel surface is responsible for the rapid potential shifts observed upon imposition of the gamma field. Upon continued radiolysis, a rise in concentration of oxidizing species (particularly H_2O_2) in the bulk solution also gradually increases the steady-state corrosion potential of the stainless steel.

4. The corrosion potential of 316L stainless steel, while sensitive to the presence of H_2O_2, does not appear to be sensitive to the presence of H_2 under our experimental conditions. While the corrosion potential is not sensitive to molecular H_2, it may be sensitive to atomic hydrogen, which is also produced under radiolysis. Molecular hydrogen may only play a role in helping to establish steady-state bulk H_2O_2 concentrations.

5. Preliminary results suggest that the susceptibility of 316L stainless steel to pitting is not increased under gamma irradiation. It appears that both the corrosion and pitting potentials are shifted positively by approximately the same amount. The more positive pitting potentials observed under gamma irradiation may be related to reaction of radiolytic products with defects (e.g., oxygen vacancies) in the oxide film, or to film-repair reactions. Further work is needed to understand the effect of gamma irradiation over wide ranges of the polarization curves.

References

1. C. J. Hochanadel, J. Phys. Chem., 56, 587 (1952).

2. J. W. T. Spinks and R. J. Woods, "An Introduction to Radiation Chemistry, 2nd edition", John Wiley and Sons, New York, 1976.

3. A. O. Allen, "The Radiation Chemistry of Water and Aqueous Solutions," D. Van Nostrand and Co., Inc., Princeton, N.J., 1961.

4. T. Furuya, T. Fukuzuka, K. Fujiwara, and H. Tomari, Kobe Res. Dev., 33, 43 (1983).

5. N. Fujita, M. Akiyama, and T. Tamura, Corrosion, 37, 335 (1981).

6. A. V. Byalobzheskii, "Radiation Corrosion", Israel Program for Scientific Translations, Jerusalem, 1970.

7. K. Ishigure, N. Fujita, T. Tamura, and K. Oshima, Nuclear Technology, 50, 169 (1980).

8. G. H. Cartledge, Nature, 186, 370 (1960).

9. S. Uchida, E. Ibe, and R. Katsura, Rad. Phys. Chem., 22, 515 (1983).

10. W. E. Clark, J. Electrochem. Soc., 105, 483 (1958).

11. W. G. Burns, W. R. Marsh, and W. S. Walters, Radiat. Phys. Chem., 21, 259 (1983).

12. J. N. Hockman and W. C. O'Neal, Lawrence Livermore National Laboratory Report UCRL-89820 Rev. 1, February 1984.

13. R. D. McCright, H. Weiss, M. C. Juhas, and R. W. Logan, Lawrence Livermore National Laboratory Report UCRL-89988, 1983.

14. W. G. Burns and P. B. Moore, Rad. Effects, 30, 233 (1976).

15. B. H. J. Bielski and J. M. Gebicki, "Species in Irradiated Oxygenated Water," Advances in Radiation Chemistry, Vol. 2, M. Burton and J. L. Magee, eds., Wiley-Interscience, New York, p. 177 (1970).

16. V. M. Oversby, Lawrence Livermore National Laboratory Report UCRL-53552, May 1984.

17. W. G. Burns, A. E. Hughes, J. A. C. Marples, R. S. Nelson, and A. M. Stoneham, Nature, 295, 130 (1982).

18. R. M. Sellers, Analyst, 105, 950 (1980).

19. C. J. Hochanadel in "Proc. U.N. Intern. Conf. Peaceful Uses At. Energy", Geneva, 1955, 7, 521, United Nations, Geneva (1955).

20. S. Gordon and E. J. Hart in "Proc. U.N. Intern. Conf. Peaceful Uses At. Energy, 2nd," Geneva, 1958, 29, 13, United Nations, Geneva (1958).

21. W. M. Latimer, "The Oxidation States of the Elements and Their Potentials in Aqueous Solution," 2nd Ed., Prentice Hall, Englewood Cliffs, N. J., 1952.

22. J. O'M. Bockris and L. F. Oldfield, Trans. Faraday Soc., 51, 249 (1955).

23. R. Gerischer and H. Gerischer, Z. Phys. Chem., 6, 178 (1956).

24. A. J. Sedriks, Corrosion of Stainless Steels, John Wiley and Sons, New York, 1979.

APPENDIX I.

Burns, et al. have developed the following equation to quantify the production of nitric acid in a sealed air/water system.[17] As a first approximation we can apply this equation to our experiments.

$$N = 2C_0R\,[1 - \exp(-1.45 \times 10^{-5}\ GDT)]$$

In this equation, N is the concentration of HNO_3 in moles ℓ^{-1}, D is the dose rate in Mrad/h^{-1}, R is the ratio of the volume of air to the volume of liquid, C_0 is the concentration of nitrogen in air in moles ℓ^{-1}, t is the time of irradiation in hours, and the G value for the reaction is 1.9.

Substituting in the approximate values in our experiments,

C_0 = 0.068 mole ℓ^{-1} (assuming dry air)
R = 0.35
G = 1.9
D = 3 Mrad/h^{-1}
t = 4 *h*

yields a value for N of 1.57×10^{-5} moles ℓ^{-1}.

TABLE 1. Measured Analyses of the Electrode Materials

Alloy	Composition (wt%)												
	C	Mn	P	S	Si	Ni	Cr	Mo	Co	Ti	Cu	Cb	N
304L	.022	1.55	.024	.025	.63	9.26	18.31	.36	.16	.002	.46	.01	.072
316L	.02	1.71	.033	.014	.56	10.29	16.51	2.07	.10	--	.28	--	.054

TABLE 2. Composition of J-13 water (average of 6 samples, by OES-ICP and IC), ppm

Al	<0.020	Si	27.0 ± 0.1
As	<0.060	Sr	0.054 ± 0.005
B	0.11 ± 0.01	U	<0.084
Be	0.003	V	0.011 ± 0.001
Cd	<0.003	Zn	<0.008
Co	<0.003	Ca	13.0 ± 0.1
Cu	<0.003	K	5.5 ± 0.3
Fe	<0.004	Mg	1.92 ± 0.01
Li	0.044 ± 0.001	Na	43.4 ± 0.3
Mn	<0.0005	Cl^-	7.1 ± 0.3
Mo	0.013 ± 0.002	F^-	2.4 ± 0.1
Ni	<0.008	NO_3^-	9.1 ± 0.2
P	<0.124	$SO_4^{=}$	18.5 ± 0.1
Pb	0.022 ± 0.003	HCO_3^-	132 ± 6
Se	<0.100		

TABLE 3. Possible Redox Reactions in Gamma-Irradiated Solutions

$H_2O + e^- \rightleftarrows e^-_{aq}$

$H^+ + e^- \rightleftarrows H\ (aq)$

$OH\ (ads) + e^- \rightleftarrows OH^-$

$OH + H^+ + e^- \rightleftarrows H_2O$

$HO_2 + H^+ + e^- \rightleftarrows H_2O_2$

$OH + e^- \rightleftarrows OH^-$

$HO_2 + 2H^+ + 2e^- \rightleftarrows H_2O + OH$

$O_2^- + H_2O + e^- \rightleftarrows HO_2^- + OH^-$

$O_2 + H^+ + e^- \rightleftarrows HO_2$

$O_2 + e^- \rightleftarrows O_2^-$

$H_2O_2 + 2H^+ + 2e^- \rightleftarrows 2H_2O$

$H_2O_2 + H^+ + e^- \rightleftarrows H_2O + OH$

$HO_2^- + H_2O + 2e^- \rightleftarrows 3OH^-$

$HO_2^- + H_2O + e^- \rightleftarrows 2OH^- + OH$

$O_2 + 2H^+ + 2e^- \rightleftarrows H_2O_2$

$O_2 + 2H_2O + 2e^- \rightleftarrows H_2O_2 + 2OH^-$

$O_2 + H_2O + 2e^- \rightleftarrows HO_2^- + OH^-$

$2H^+ + 2e^- \rightleftarrows H_2$

$2H_2O + 2e^- \rightleftarrows H_2 + 2OH^-$

$O_2 + 4H^+ + 4e^- \rightleftarrows 2H_2O$

$O_2 + 2H_2O + 4e^- \rightleftarrows 4OH^-$

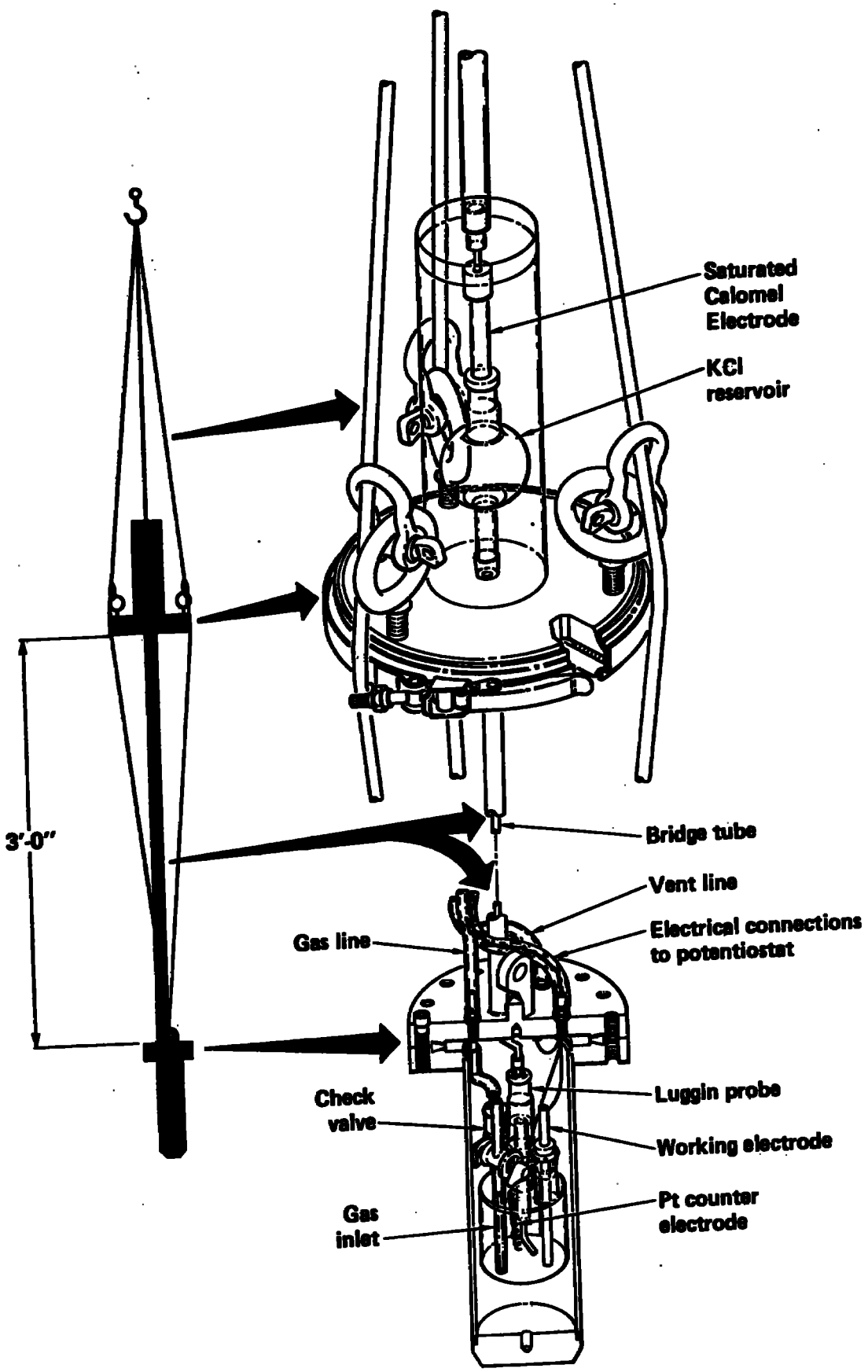

Figure 1: Schematic of the electrochemical cell used in this work. Details are provided in the text.

Figure 2: Corrosion potential behavior for 316L stainless steel in 10X concentrated J-13 well water under gamma irradiation. The solution was not exposed to irradiation prior to initiation of the first "on/off" irradiation cycle.

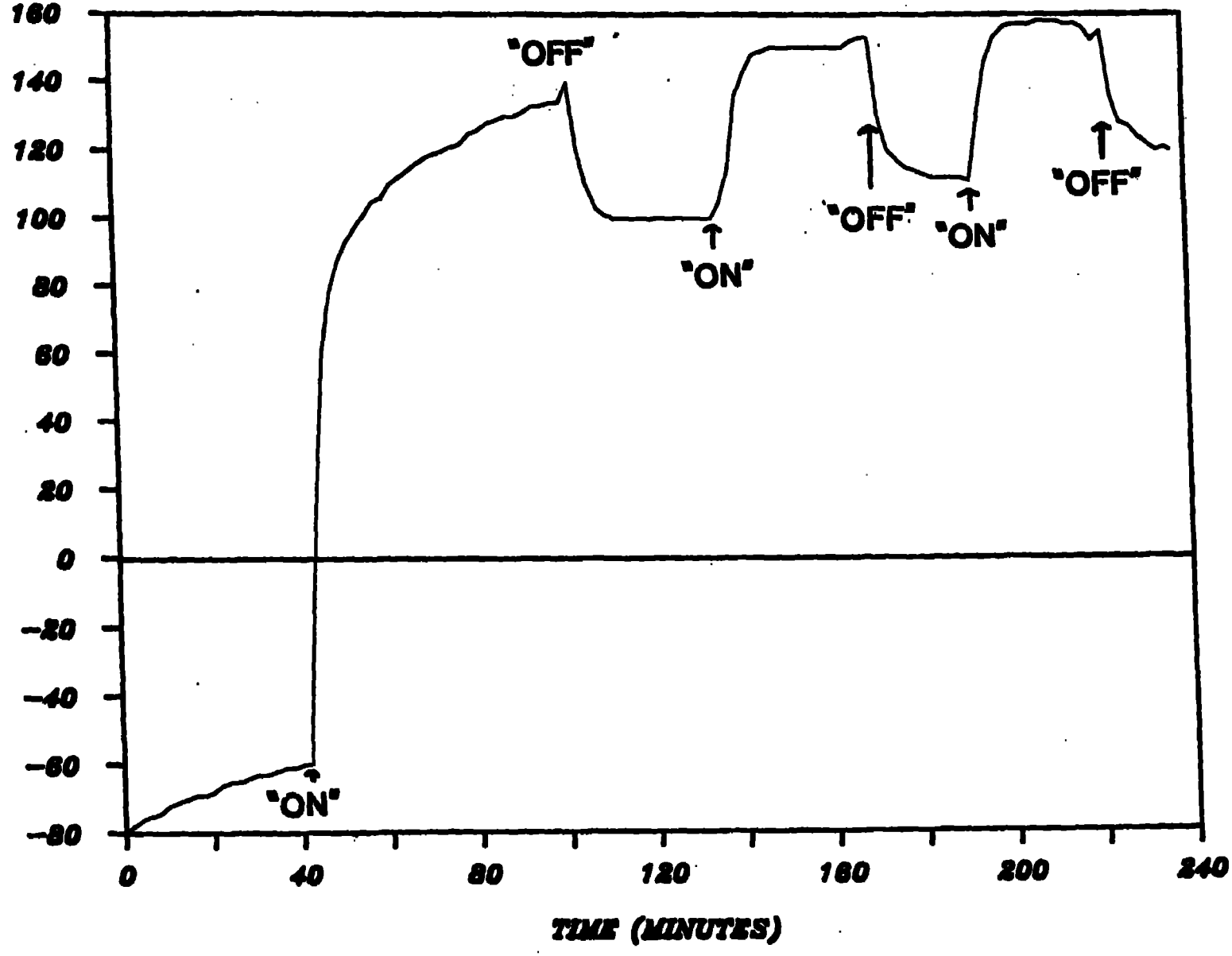

Figure 3: As for Figure 2, only for a 100X concentrated J-13 electrolyte.

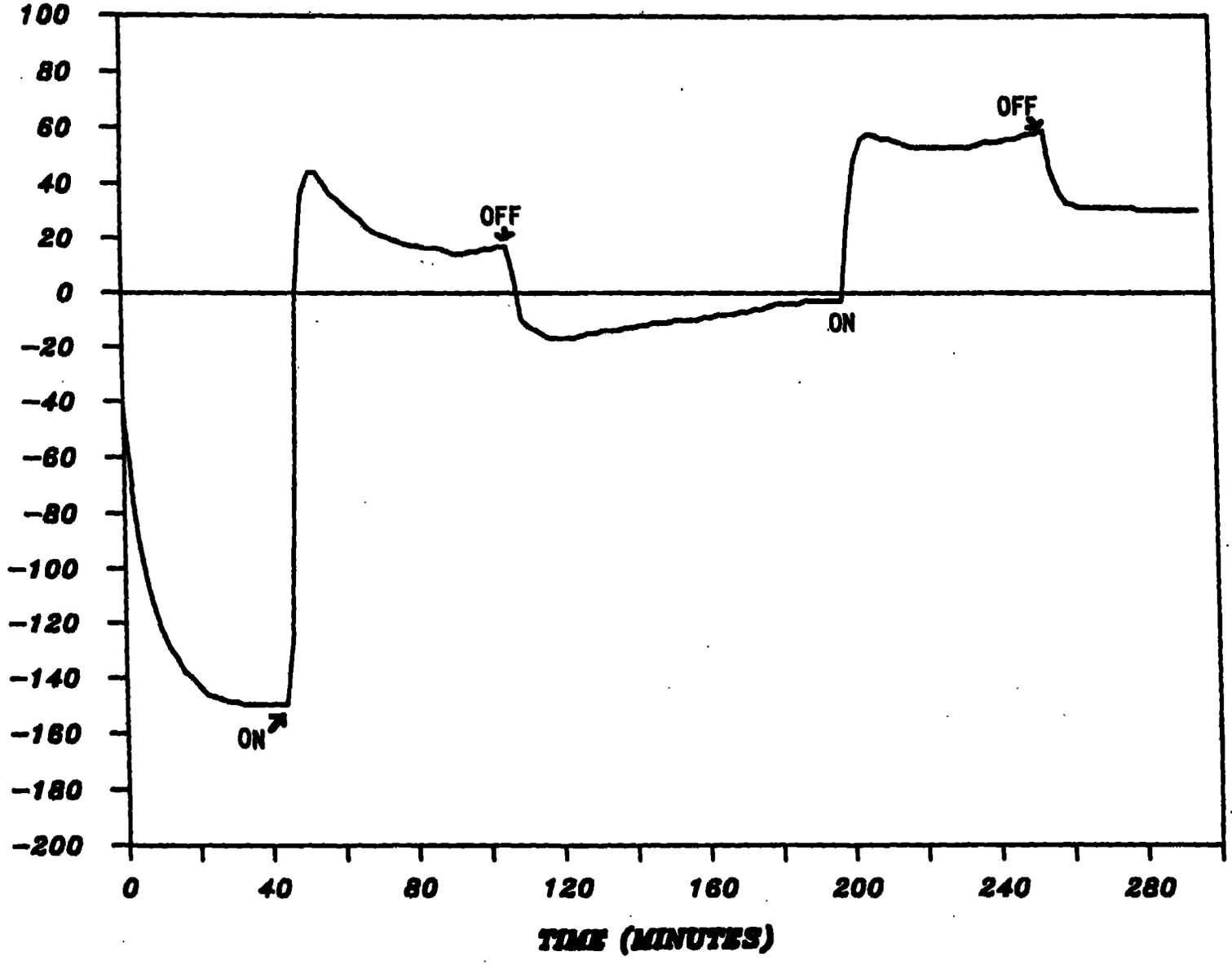

Figure 4: Corrosion potential behavior for 316L stainless steel in gamma-irradiated J-13 well water. Following the last "off" half-cycle the irradiated solution was decanted and replaced by a fresh, unirradiated solution. Following this, two drops of H_2O_2 (from a 30% solution) were added successively. One drop of H_2O_2 represents a resulting solution concentration of 4.4 mM.

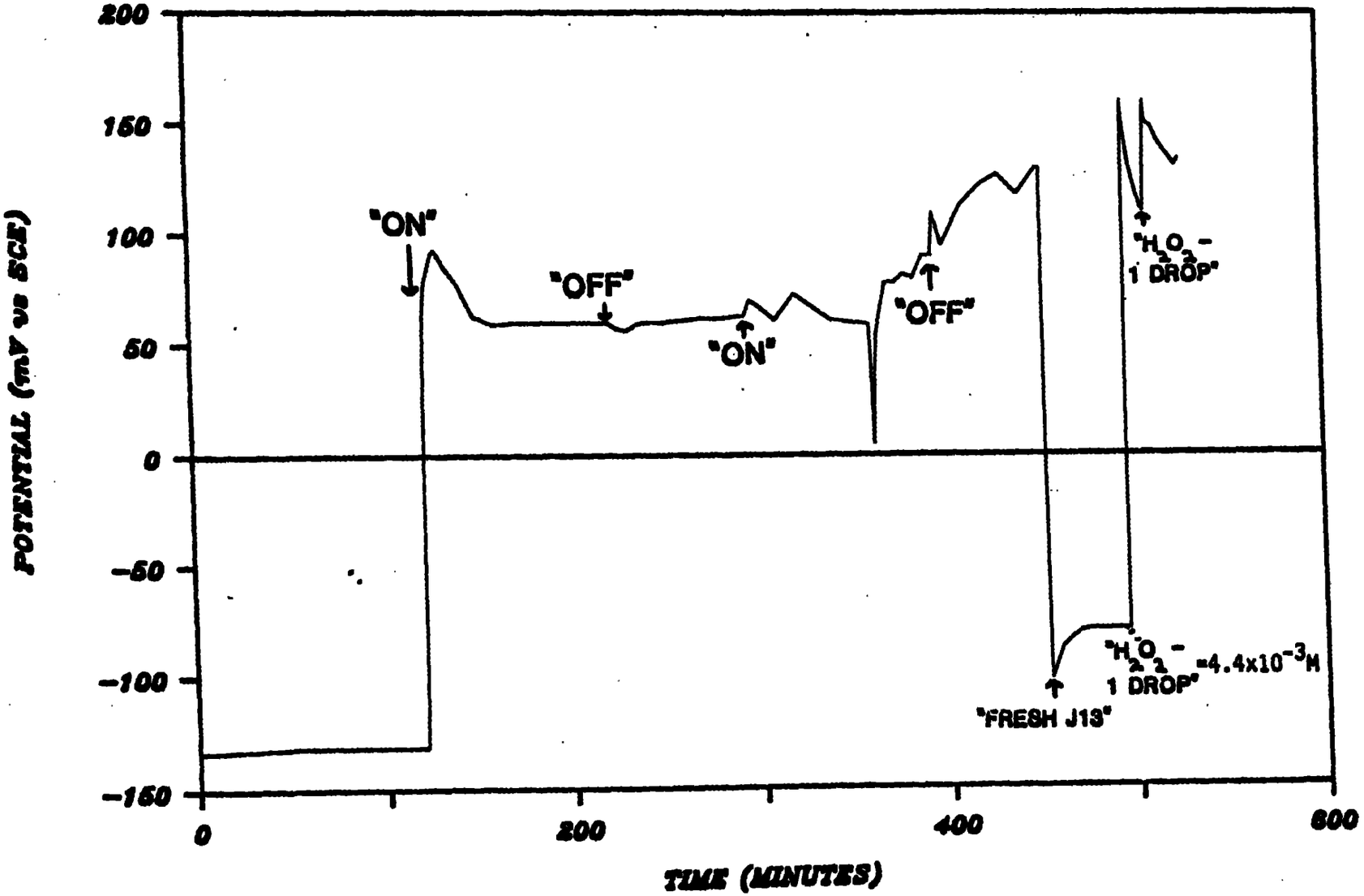

Figure 5: Response of the corrosion potential for 316L stainless steel in J-13 well water to which successive additions of H_2O_2 were made. In this figure, one drop of H_2O_2 (from a 30% solution) represents a resulting solution concentration of 0.49 mM. The solution was continuously stirred by a magnetic stirrer throughout the experiment.

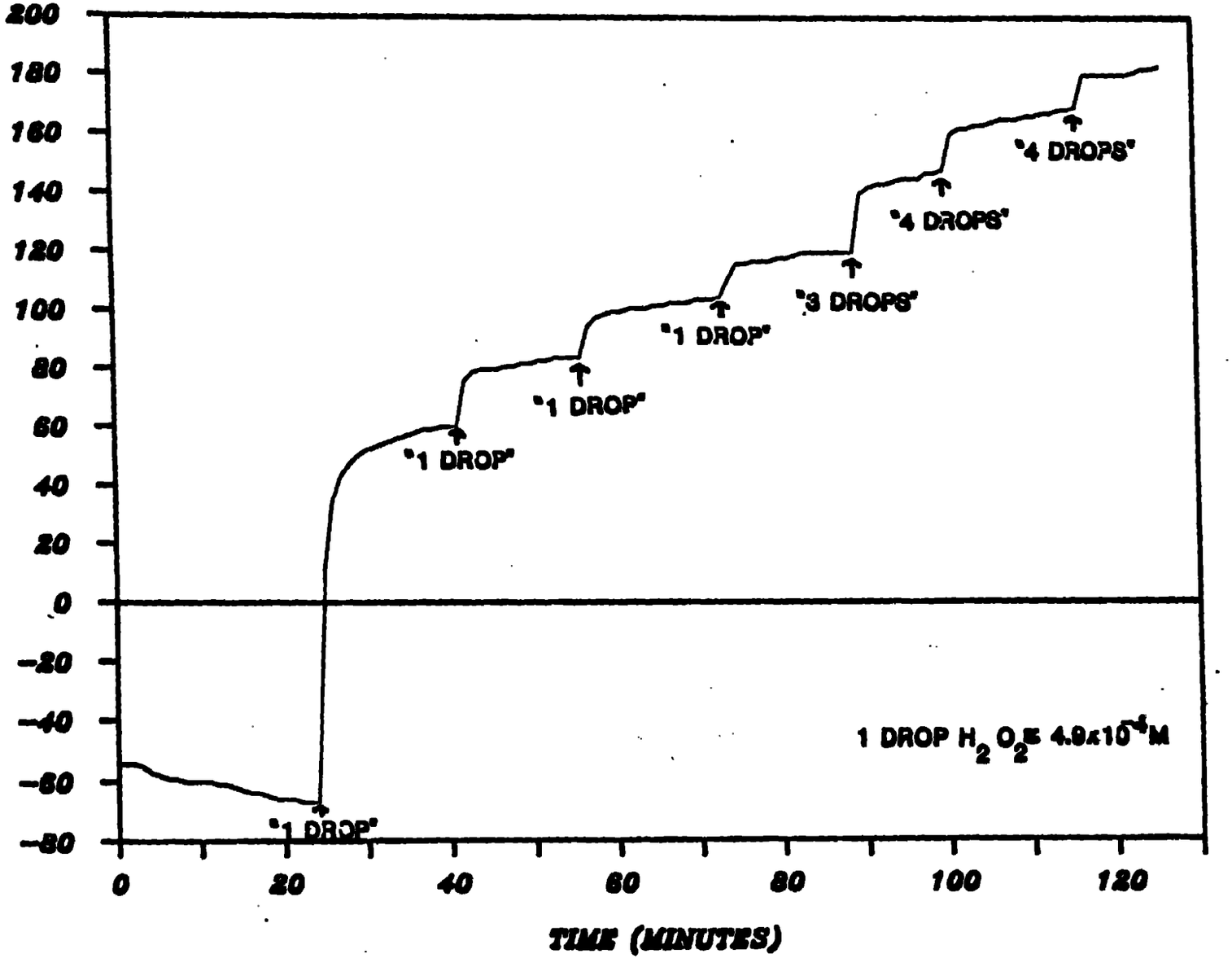

Figure 7: As for Figure 6, only with continuous purging of the solution by argon throughout the experiment.

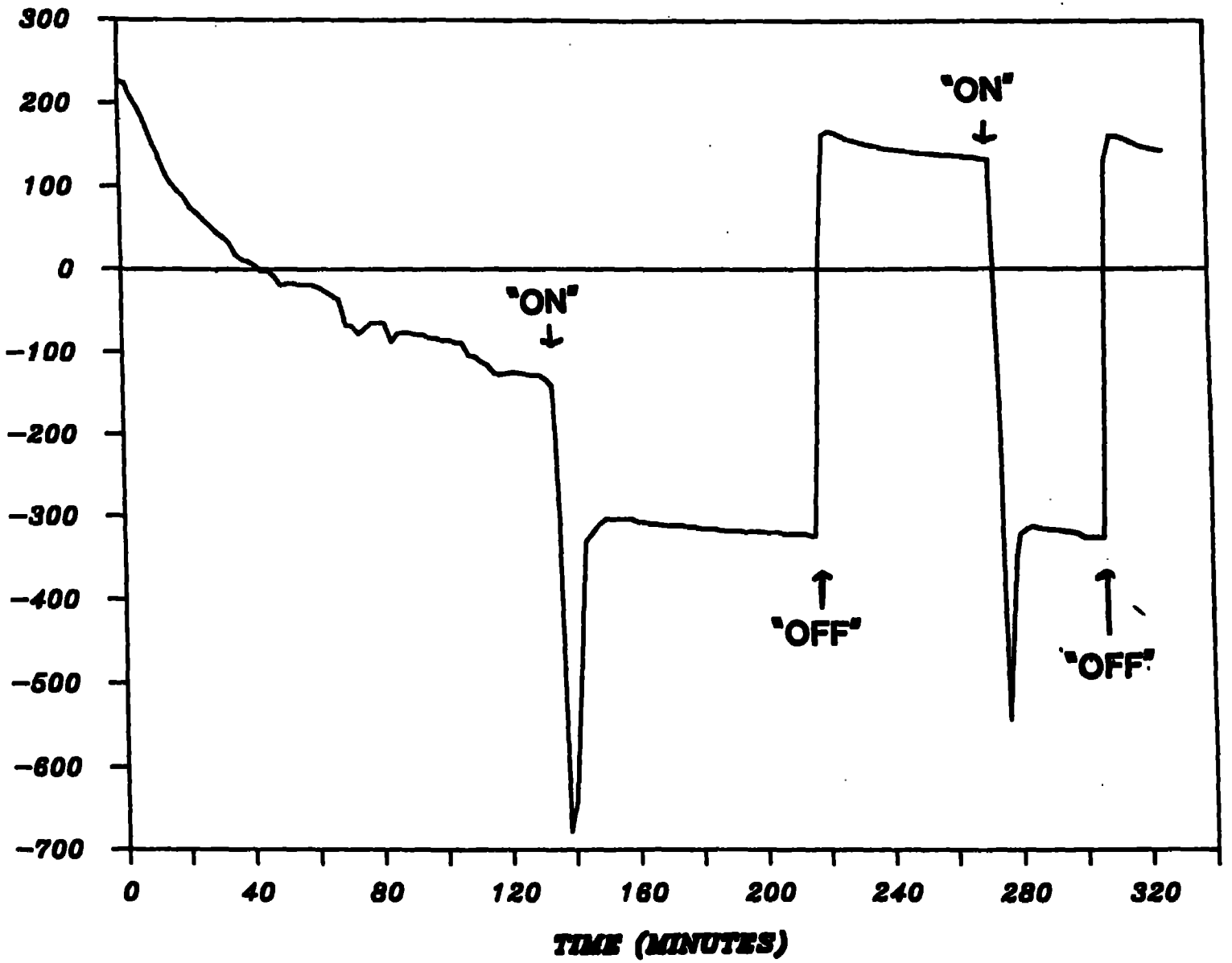

Figure 7: As for Figure 6, only with continuous purging of the solution by argon throughout the experiment.

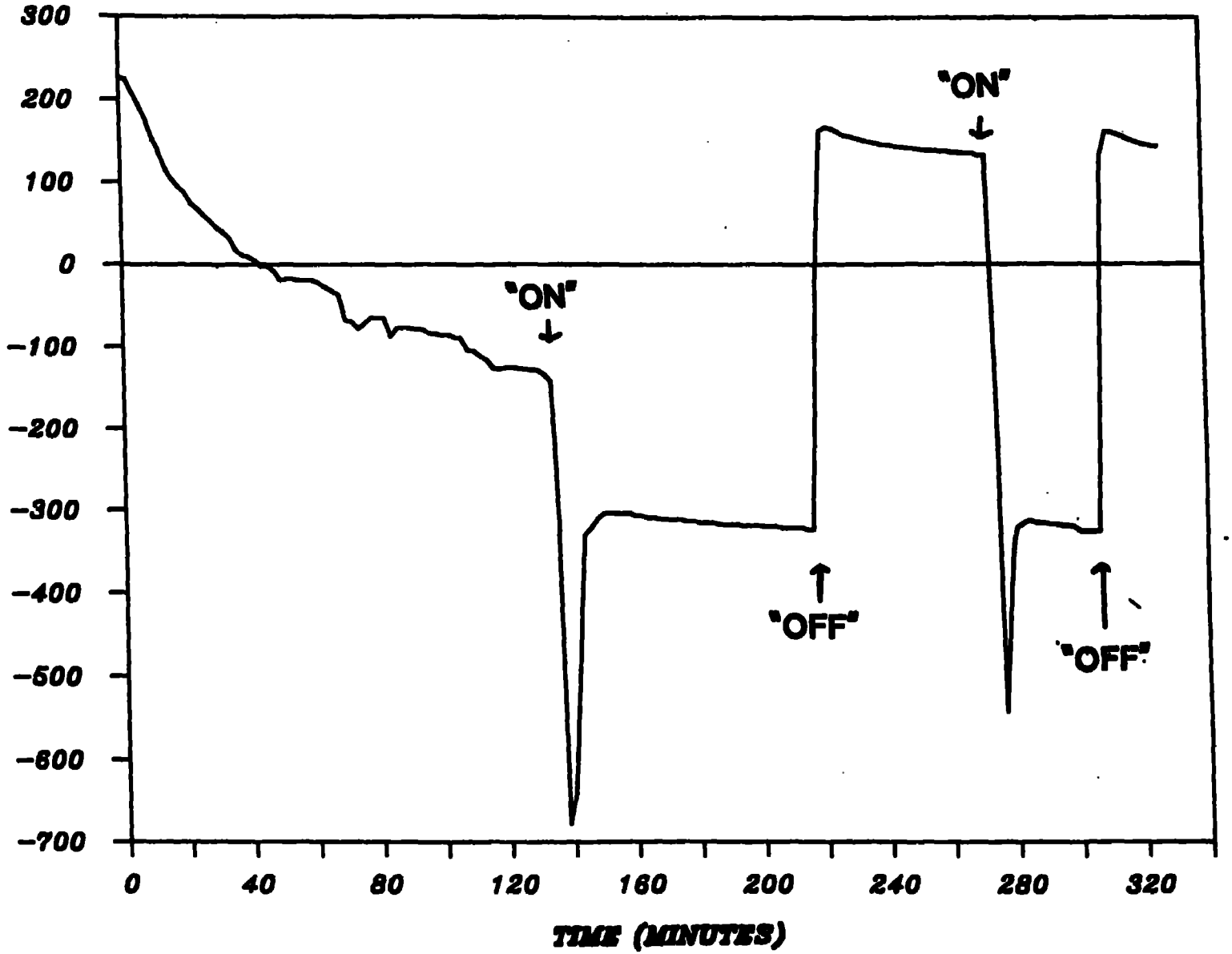

Figure 8: Response of the open-circuit potential for platinum in unirradiated J-13 well water to successive additions of H_2, H_2O_2, and O_2. The points of introduction of these species into solution are indicated on the figure. In this figure, two drops of H_2O_2 (from a 30% solution) results in a solution concentration of 0.98 mM. Purging of the solution with H_2 and O_2 resulted in successive saturated solutions of these gases. The solution was continuously stirred by a magnetic stirrer during the experiment.

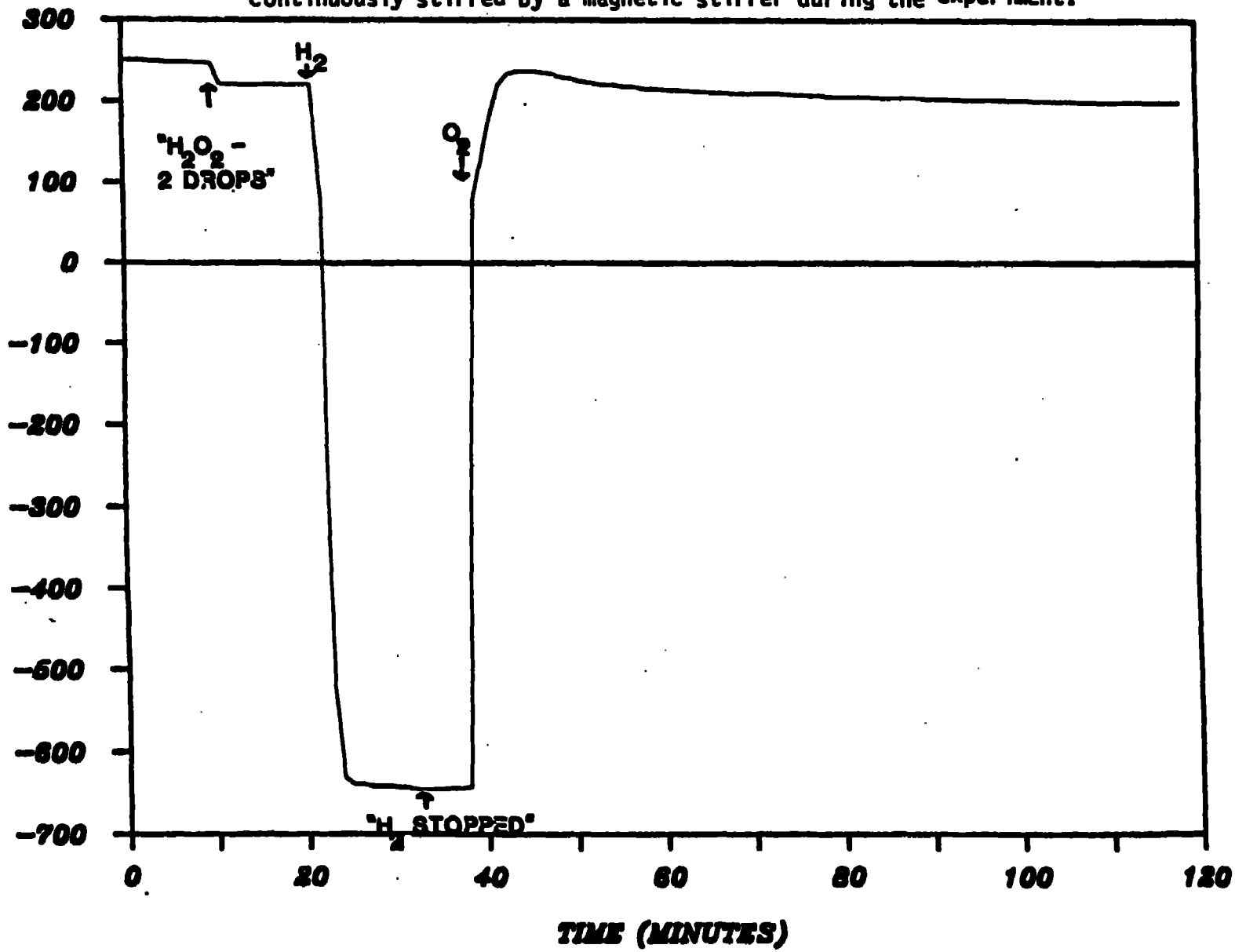

Figure 9: Response of the corrosion potential for 316L stainless steel in J-13 well water to successive additions of H_2O_2 and H_2. The points of introduction of these species into solution are indicated on the figure. In this experiment the addition of two drops of H_2O_2 (from a 30% solution) resulted in a solution concentration of 0.98 mM. Purging of the solution with H_2 saturated the solution with H_2. The solution was continuously stirred with a magnetic stirrer in this experiment.

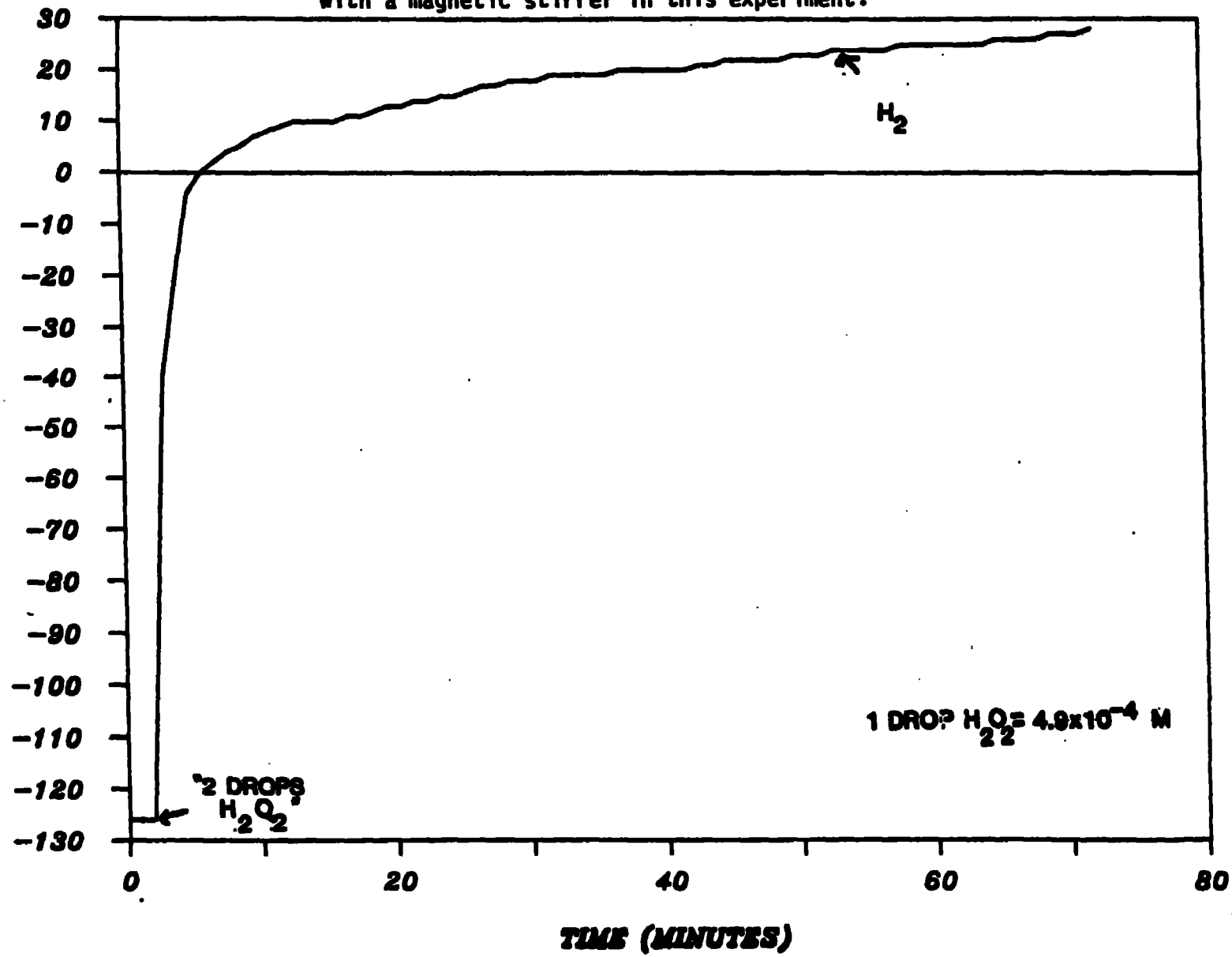

Figure 10: Response of the corrosion potential for 316L stainless steel in argon-purged J-13 well water to gamma irradiation. Initiation of argon deaeration and gamma irradiation are indicated on the figure. Once initiated, argon purging was continued throughout the remainder of the experiment.

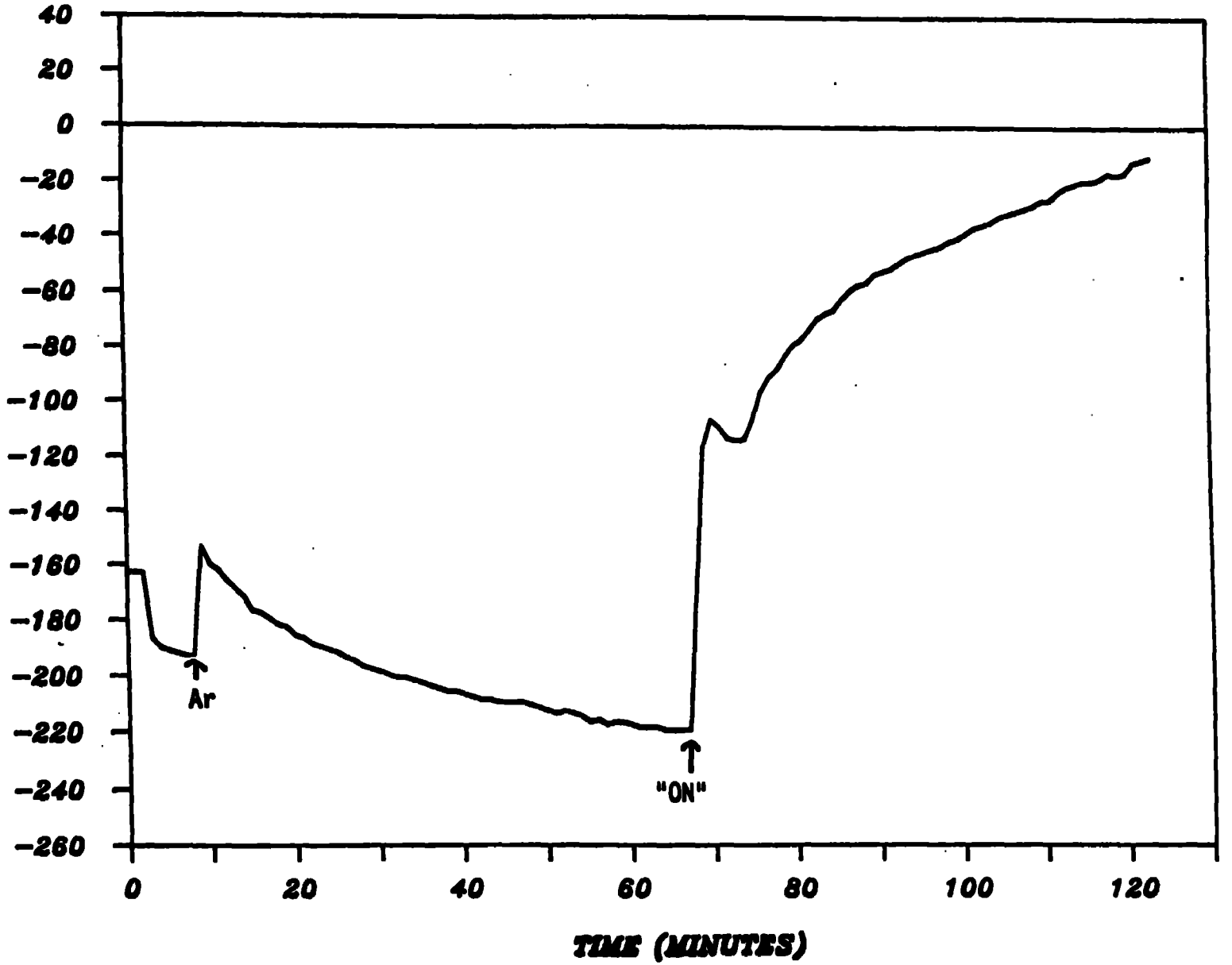

Figure 11: Comparison of the potentiostatic anodic polarization behavior for 316L stainless steel in 650 ppm Cl^- solution in deionized water with and without gamma irradiation. The polarization curves were scanned anodically starting from the corrosion potential in each case. Upon reaching the anodic limit, the scans were reversed to more negative potentials. In this figure, E_{corr} and E_p represent values of the corrosion potential and pitting potential, respectively, for the unirradiated case. The corresponding values for the irradiated experiment are indicated on the figure as $^*E_{corr}$ and $^*E_p$.